

Trust Region Masking for Long-Horizon LLM Reinforcement Learning

Yingru Li*, Jiakai Liu^{*1}, Jiawei Xu^{*2}, Yuxuan Tong, Ziniu Li²,
Qian Liu, and Baoxiang Wang²

¹Fudan University, ²The Chinese University of Hong Kong, Shenzhen

Abstract

Policy gradient methods for Large Language Models optimize a policy π_θ via a surrogate objective computed from samples of a rollout policy π_{roll} . However, modern LLM-RL pipelines suffer from unavoidable implementation divergences—backend discrepancies, Mixture-of-Experts routing discontinuities, and distributed training staleness—causing off-policy mismatch ($\pi_{\text{roll}} \neq \pi_\theta$) and approximation errors between the surrogate and the true objective. We demonstrate that classical trust region bounds on this error scale as $O(T^2)$ with sequence length T , rendering them vacuous for long-horizon tasks. To address this, we derive a family of bounds—both KL-based and TV-based—including a *Pinsker-Marginal* bound ($O(T^{3/2})$), a *Mixed* bound ($O(T)$), and an *Adaptive* bound that strictly generalizes the Pinsker-Marginal bound via per-position importance-ratio decomposition. Taking the minimum over all bounds yields the tightest known guarantee across all divergence regimes. Crucially, all bounds depend on the maximum token-level divergence $D_{\text{KL}}^{\text{tok,max}}$ (or $D_{\text{TV}}^{\text{tok,max}}$), a *sequence-level* quantity that cannot be controlled by token-independent methods like PPO clipping. We propose Trust Region Masking (TRM), which masks entire sequences violating the trust region, enabling the first non-vacuous monotonic improvement guarantees for long-horizon LLM-RL.

1 Introduction

Reinforcement Learning (RL) has become central to training Large Language Models (LLMs) for tasks requiring extended reasoning, multi-step problem solving, and agentic behavior [Zeng et al., 2025, Liu et al., 2024b, Yang et al., 2024]. As response lengths expand from hundreds to thousands of tokens, policy gradient methods—particularly PPO [Schulman et al., 2017]—face increasingly strained theoretical foundations.

Trust region methods [Kakade and Langford, 2002, Schulman et al., 2015] provide monotonic improvement guarantees by bounding the approximation error $|J(\pi_\theta) - J(\pi_{\text{roll}}) - L(\pi_\theta)|$ between the true objective J and the surrogate L . This guarantee requires controlling the divergence between the rollout policy π_{roll} and the training policy π_θ —a divergence that is *unavoidable* in modern LLM-RL due to three primary sources. **(i) Backend discrepancies:** high-throughput inference engines (vLLM [Kwon et al., 2023], SGLang [Zheng et al., 2024]) use different attention kernels, precision formats, and operator fusion strategies than training frameworks (Megatron-LM [Shoeybi et al., 2019], PyTorch FSDP [Zhao et al., 2023]), causing logit differences that compound autoregressively. **(ii) MoE routing discontinuities:** in Mixture-of-Experts models [Shazeer et al., 2017, Liu et al.,

*Equal contribution

2024a], minor numerical jitter can flip expert selection, causing high-magnitude jumps in token probabilities. **(iii) Distributed staleness:** asynchronous actor-learner architectures [Espeholt et al., 2018, Nair et al., 2015] introduce latency between data generation and gradient updates. These factors are documented in detail by Liu et al. [2025] and Yao et al. [2025]; we provide further analysis in Appendix A.

Classical trust region bounds [Kakade and Langford, 2002, Achiam et al., 2017] scale as $O(T^2)$ with sequence length. For a reasoning task with $T = 4096$ tokens and per-token divergence $D_{\text{KL}}^{\text{tok,max}} = 10^{-4}$, the classical bound yields $|\text{Error}| \leq 1677$ —vacuous given maximum reward of 1. While acceptable for short-horizon control tasks ($T \approx 100$), these bounds provide no guarantee that optimization actually improves performance at modern LLM scales.

Standard PPO addresses trust regions through token-level clipping [Ziegler et al., 2019], but autoregressive generation is inherently sequential: a small probability shift at an early token compounds through the entire trajectory, a phenomenon related to “exposure bias” [Bengio et al., 2015]. Distributed RL frameworks like IMPALA [Espeholt et al., 2018] introduce correction mechanisms for staleness, but do not address the fundamental $O(T^2)$ scaling of the approximation error. Our work bridges this gap by deriving tight, non-vacuous bounds for autoregressive sequence generation and proposing sequence-level masking to enforce them.

We make the following contributions:

1. **A family of tighter bounds (Section 3):** We derive KL-based and TV-based variants of three bound families—Pinsker-Marginal ($O(T^{3/2})$), Mixed ($O(T)$), and Adaptive—and show that their minimum is the tightest known guarantee across all divergence regimes (Theorem 3.8).
2. **Trust Region Masking (Section 4):** We show that all bounds depend on the maximum token-level divergence—a sequence-level quantity uncontrollable by token-level PPO clipping—and propose TRM, which masks entire sequences violating the trust region, enabling non-vacuous monotonic improvement guarantees. We demonstrate empirical training stability on mathematical reasoning benchmarks.

2 Background and Problem Setup

2.1 Autoregressive Generation and Objective

A policy π_θ generates a response $y = (y_1, \dots, y_T)$ given prompt x , with trajectory probability $P^{\pi_\theta}(y \mid x) = \prod_{t=1}^T \pi_\theta(y_t \mid x, y_{<t})$. We define the context $c_t = (x, y_{<t})$ and the context visitation distribution:

$$d_t^\pi(c_t) = P(x) \prod_{s=1}^{t-1} \pi(y_s \mid c_s). \quad (1)$$

Given a scalar reward $R(x, y) \in [0, 1]$, the objective is $J(\pi_\theta) = \mathbb{E}_{x \sim P(x), y \sim \pi_\theta(\cdot \mid x)}[R(x, y)]$.

2.2 The Surrogate Objective

Samples are generated from a rollout policy π_{roll} that generally differs from π_θ . Following Kakade and Langford [2002], we define the surrogate:

$$L_{\pi_{\text{roll}}}(\pi_\theta) = \mathbb{E}_{\pi_{\text{roll}}} \left[A \cdot \sum_{t=1}^T \rho_t \right], \quad (2)$$

where $A = R(x, y) - b$ is the trajectory advantage (with baseline b), $\rho_t = \pi_\theta(y_t | c_t) / \pi_{\text{roll}}(y_t | c_t)$ is the per-token importance ratio, and the gradient matches the true gradient at the reference: $\nabla L_{\pi_{\text{roll}}}(\pi_\theta)|_{\pi_\theta = \pi_{\text{roll}}} = \nabla J(\pi_\theta)|_{\pi_\theta = \pi_{\text{roll}}}$. The approximation error is:

$$\text{Error}(\pi_\theta) := J(\pi_\theta) - J(\pi_{\text{roll}}) - L(\pi_\theta). \quad (3)$$

Bounding $|\text{Error}|$ guarantees that maximizing L leads to monotonic improvement in J .

Remark 2.1 (Surrogate equivalence). *The error analysis uses the equivalent form $L'_{\pi_{\text{roll}}}(\pi_\theta) = \mathbb{E}_{\pi_{\text{roll}}}[R(x, y) \sum_t (\rho_t - 1)]$. Any fixed baseline b contributes a π_θ -independent constant that does not affect Error, so all bounds apply equally to both forms.*

2.3 Divergence Measures

We employ two families of divergence measures throughout.

Definition 2.2 (Token-level divergences). *For context $c_t = (x, y_{<t})$:*

$$D_{\text{TV}}^{\text{tok}}(c_t) := D_{\text{TV}}(\pi_\theta(\cdot | c_t) \| \pi_{\text{roll}}(\cdot | c_t)) = \frac{1}{2} \sum_v |\pi_\theta(v | c_t) - \pi_{\text{roll}}(v | c_t)|, \quad (4)$$

$$D_{\text{KL}}(c_t) := D_{\text{KL}}(\pi_{\text{roll}}(\cdot | c_t) \| \pi_\theta(\cdot | c_t)) = \sum_v \pi_{\text{roll}}(v | c_t) \log \frac{\pi_{\text{roll}}(v | c_t)}{\pi_\theta(v | c_t)}. \quad (5)$$

Definition 2.3 (Sequence-level divergences). *We define the maximum token-level divergences, the sequence-level divergences, and the expected per-position TV:*

$$\epsilon := D_{\text{TV}}^{\text{tok, max}} := \max_{t, c_t} D_{\text{TV}}^{\text{tok}}(c_t), \quad \delta := D_{\text{KL}}^{\text{tok, max}} := \max_{t, c_t} D_{\text{KL}}(c_t), \quad (6)$$

$$D_{\text{TV}}^{\text{seq}} := D_{\text{TV}}(P^{\pi_{\text{roll}}}(\cdot | x) \| P^{\pi_\theta}(\cdot | x)), \quad D_{\text{KL}}^{\text{seq}} := \sum_{t=1}^T \mathbb{E}_{c_t \sim d_t^{\pi_{\text{roll}}}} [D_{\text{KL}}(c_t)], \quad (7)$$

$$\bar{D}_t := \mathbb{E}_{c_t \sim d_t^{\pi_{\text{roll}}}} [D_{\text{TV}}^{\text{tok}}(c_t)]. \quad (8)$$

The key relationships between these quantities are (proofs in Appendix B):

- **Pinsker’s inequality:** $D_{\text{TV}}^{\text{tok}}(c_t) \leq \min(1, \sqrt{D_{\text{KL}}(c_t)/2})$, and therefore $\epsilon \leq \min(1, \sqrt{\delta/2})$.
- **KL chain rule:** $D_{\text{KL}}(d_t^{\pi_{\text{roll}}} \| d_t^{\pi_\theta}) = \sum_{s=1}^{t-1} \mathbb{E}_{c_s \sim d_s^{\pi_{\text{roll}}}} [D_{\text{KL}}(c_s)] \leq (t-1) \delta$.
- **Data processing inequality:** $\|d_t^{\pi_\theta} - d_t^{\pi_{\text{roll}}}\|_{\text{TV}} \leq D_{\text{TV}}^{\text{seq}}$.

Pinsker is *tight* when the two distributions differ uniformly across the vocabulary, and *loose* when divergence is concentrated on a few tokens (e.g., MoE routing flips). This motivates maintaining TV-based bounds alongside KL-based bounds: the KL route exploits sublinear context-shift scaling via Pinsker, while the TV route avoids Pinsker’s looseness.

3 Theoretical Analysis

We derive a family of bounds on $|\text{Error}|$ using both KL-based and TV-based routes. All proofs are in Appendix C.

3.1 Building Blocks

The error decomposes via the Performance Difference Identity [Kakade and Langford, 2002]. Let $A_t^{\pi_{\text{roll}}}(c_t, y_t) := \mathbb{E}_{\pi_{\text{roll}}}[R \mid c_t, y_t] - \mathbb{E}_{\pi_{\text{roll}}}[R \mid c_t]$ be the per-step advantage and $g_t(c_t) := \mathbb{E}_{y_t \sim \pi_\theta}[A_t^{\pi_{\text{roll}}}(c_t, y_t)]$ the expected advantage shift. Then:

$$\text{Error} = \sum_{t=1}^T \left(\mathbb{E}_{c_t \sim d_t^{\pi_\theta}}[g_t(c_t)] - \mathbb{E}_{c_t \sim d_t^{\pi_{\text{roll}}}}[g_t(c_t)] \right). \quad (9)$$

Each summand is bounded via $|\mathbb{E}_P[f] - \mathbb{E}_Q[f]| \leq 2\|f\|_\infty \cdot D_{\text{TV}}(P, Q)$. Two building blocks control the factors:

Lemma 3.1 (Advantage Bound). *For $R \in [0, 1]$: $\|g_t\|_\infty \leq 2 \min(1, \epsilon, \sqrt{\delta/2})$.*

Lemma 3.2 (Context Shift). *The context distribution shift is bounded by:*

$$\|d_t^{\pi_\theta} - d_t^{\pi_{\text{roll}}}\|_{\text{TV}} \leq \min \left(1, \underbrace{(t-1)\epsilon}_{\text{coupling}}, \underbrace{\sqrt{(t-1)\delta/2}}_{\text{Pinsker-on-marginal-KL}}, \underbrace{D_{\text{TV}}^{\text{seq}}}_{\text{data processing}}, \underbrace{\sqrt{D_{\text{KL}}^{\text{seq}}/2}}_{\text{Pinsker-on-seq-KL}} \right). \quad (10)$$

Choosing different combinations of these building blocks yields different bound families.

The Classical Bound and Its Failure Using $\|g_t\|_\infty \leq 2\epsilon$ with the coupling bound $(t-1)\epsilon$ and no caps:

$$|\text{Error}| \leq 4\epsilon^2 \sum_{t=1}^T (t-1) = 2T(T-1)\epsilon^2. \quad (11)$$

Since $\epsilon \leq \sqrt{\delta/2}$, this implies $|\text{Error}| \leq T(T-1)\delta$. At $T = 4096$, $\delta = 10^{-4}$: $|\text{Error}| \leq 4096 \times 4095 \times 10^{-4} \approx 1677$ —*vacuous*.

3.2 New Tighter Bounds

Pinsker-Marginal Bounds Applying Pinsker’s inequality to the *marginal* KL gives a sublinear context shift $\sqrt{(t-1)\delta/2}$, while the advantage factor can use either the KL-derived bound $\sqrt{\delta/2}$ or the direct TV value ϵ :

Theorem 3.3 (Pinsker-Marginal Bounds).

$$B_{\text{PM}}^{\text{KL}} = 4 \min \left(1, \sqrt{\frac{\delta}{2}} \right) \sum_{t=1}^T \min \left(1, \sqrt{\frac{(t-1)\delta}{2}} \right), \quad (12)$$

$$B_{\text{PM}}^{\text{TV}} = 4 \min(1, \epsilon) \sum_{t=1}^T \min \left(1, \sqrt{\frac{(t-1)\delta}{2}} \right). \quad (13)$$

In the small-divergence regime ($\delta \leq 2/T$, so all caps are inactive):

$$B_{\text{PM}}^{\text{KL}} = \frac{4}{3}T^{3/2}\delta, \quad B_{\text{PM}}^{\text{TV}} = \frac{8}{3}T^{3/2}\epsilon\sqrt{\delta/2}. \quad (14)$$

The TV variant replaces $\sqrt{\delta/2}$ with ϵ in the advantage factor, gaining whenever Pinsker is loose ($\epsilon < \sqrt{\delta/2}$). When Pinsker is tight ($\epsilon = \sqrt{\delta/2}$), both variants coincide.

Mixed Bounds Using a *uniform* context-shift bound from the sequence-level divergence (which does not grow with t):

Theorem 3.4 (Mixed Bounds).

$$B_{\text{Mix}}^{\text{KL}} = 4T \cdot \min\left(1, \sqrt{\frac{\delta}{2}}\right) \cdot \min\left(1, \sqrt{\frac{D_{\text{KL}}^{\text{seq}}}{2}}\right), \quad (15)$$

$$B_{\text{Mix}}^{\text{TV}} = 4T \cdot \min(1, \epsilon) \cdot \min(1, D_{\text{TV}}^{\text{seq}}). \quad (16)$$

When both caps are inactive: $B_{\text{Mix}}^{\text{KL}} = 2T\sqrt{\delta \cdot D_{\text{KL}}^{\text{seq}}}$ and $B_{\text{Mix}}^{\text{TV}} = 4T\epsilon D_{\text{TV}}^{\text{seq}}$.

The Mixed bounds scale as $O(T)$ and are tighter when divergence is sparse ($D_{\text{KL}}^{\text{seq}} \ll T\delta$).

Coupling Bounds The pure TV-coupling route avoids all KL/Pinsker conversions:

Theorem 3.5 (Coupling Bound).

$$B_{\text{Coup}} = 4 \min(1, \epsilon) \sum_{t=1}^T \min(1, (t-1)\epsilon). \quad (17)$$

When $T\epsilon \leq 1$: $B_{\text{Coup}} = 2T(T-1)\epsilon^2$ (classical). When $T\epsilon > 1$: $B_{\text{Coup}} \leq 4T\epsilon$ ($O(T)$ via the cap).

Adaptive Bounds The preceding bounds use worst-case advantage terms (ϵ or $\sqrt{\delta/2}$). The Adaptive bound preserves the data-dependent per-position divergence \bar{D}_t via an importance-ratio decomposition (full derivation in Appendix D).

Theorem 3.6 (Adaptive Bounds).

$$B_{\text{Adap}}^{\text{KL}} = 4 \sum_{t=1}^T \bar{D}_t \cdot \min\left(1, \sqrt{\frac{(T-t)\delta}{2}}\right), \quad (18)$$

$$B_{\text{Adap}}^{\text{TV}} = 4 \sum_{t=1}^T \bar{D}_t \cdot \min(1, (T-t)\epsilon), \quad (19)$$

$$B_{\text{Adap}}^* = 4 \sum_{t=1}^T \bar{D}_t \cdot \min\left(1, (T-t)\epsilon, \sqrt{\frac{(T-t)\delta}{2}}\right). \quad (20)$$

The hybrid bound $B_{\text{Adap}}^* \leq \min(B_{\text{Adap}}^{\text{KL}}, B_{\text{Adap}}^{\text{TV}})$ by construction.

The Adaptive bounds are tighter than the Pinsker-Marginal and Coupling bounds in two independent ways:

1. **Data-dependent advantage:** \bar{D}_t (expected per-position TV under π_{roll}) replaces ϵ or $\sqrt{\delta/2}$ (worst-case). When divergence is non-uniform—e.g., concentrated at a few tokens due to MoE routing— $\bar{D}_t \ll \epsilon$ at most positions.
2. **Adaptive future bounding:** The future-trajectory TV is bounded by the tighter of two routes at each position. The Pinsker route gives $\sqrt{(T-t)\delta/2}$ (sublinear in remaining horizon); the coupling route gives $(T-t)\epsilon$ (linear but avoids Pinsker looseness). The crossover occurs at $T-t = \delta/(2\epsilon^2)$.

Remark 3.7 (Recovery of prior bounds). Setting $\bar{D}_t = \min(1, \sqrt{\delta/2})$ in $B_{\text{Adap}}^{\text{KL}}$ recovers $B_{\text{PM}}^{\text{KL}}$ exactly (via the index reversal $\sum_t f(T-t) = \sum_t f(t-1)$). Setting $\bar{D}_t = \epsilon$ in $B_{\text{Adap}}^{\text{TV}}$ recovers B_{Coup} exactly. Since $\bar{D}_t \leq \min(1, \epsilon, \sqrt{\delta/2})$ always, the Adaptive bounds are at least as tight and strictly tighter when divergence is non-uniform.

Table 1: Error bounds for $T = 4096$. **Small divergence:** $\delta = 10^{-4}$, $\epsilon = 5 \times 10^{-3}$ (actual TV $< \sqrt{\delta/2} \approx 7.07 \times 10^{-3}$, so Pinsker is loose), $D_{\text{KL}}^{\text{seq}} = 0.01$, $D_{\text{TV}}^{\text{seq}} = 0.05$. **KL-only:** same δ and $D_{\text{KL}}^{\text{seq}}$, with ϵ and $D_{\text{TV}}^{\text{seq}}$ derived via Pinsker ($\epsilon = 7.07 \times 10^{-3}$, $D_{\text{TV}}^{\text{seq}} = 0.0707$), showing that TV bounds reduce to KL bounds. The unified bound B^* (bottom row) takes the minimum over all rows.

Bound	Route	Scaling	KL-only	KL+TV
Classical	TV (uncapped)	$O(T^2)$	1,677	839
Coupling	TV coupling (capped)	$O(T)^\dagger$	113.8	79.9
Pinsker-Marginal	KL	$O(T^{3/2})$	35.0	35.0
Pinsker-Marginal	TV+KL	$O(T^{3/2})$	35.0	24.7
Mixed	KL	$O(T)$	8.2	8.2
Mixed	TV	$O(T)$	8.2	4.1
Adaptive (hybrid)	KL+TV	data-dep.	$\leq 35.0^*$	$\leq 24.7^*$
Unified B^*	min all	—	≤ 8.2	≤ 4.1

$^\dagger O(T^2)$ without caps; $O(T)$ when $T\epsilon > 1$ and the $\min(1, \cdot)$ cap activates. * Worst-case Adaptive hybrid (uniform \bar{D}_t): reduces to PM-KL when $\epsilon = \sqrt{\delta/2}$, and to PM-TV when $\epsilon < \sqrt{\delta/2}$. Strictly tighter with non-uniform \bar{D}_t .

3.3 The Unified Bound

Since all bounds hold independently, their minimum is valid:

Theorem 3.8 (Unified Bound). *The approximation error satisfies $|\text{Error}| \leq B^*$, where:*

$$B^* = \min \left\{ B_{\text{PM}}^{\text{KL}}, B_{\text{PM}}^{\text{TV}}, B_{\text{Mix}}^{\text{KL}}, B_{\text{Mix}}^{\text{TV}}, B_{\text{Coup}}, B_{\text{Adap}}^* \right\}. \quad (21)$$

Defining $\mathcal{M}(\pi_\theta) := L(\pi_\theta) - B^*$, the condition $\mathcal{M}(\pi_\theta) > 0$ guarantees monotonic improvement: $J(\pi_\theta) > J(\pi_{\text{roll}})$.

All bounds depend on token-level maxima. Whether parameterized by $\delta = D_{\text{KL}}^{\text{tok}, \max}$ or $\epsilon = D_{\text{TV}}^{\text{tok}, \max}$, every bound depends on the worst-case per-token divergence. Controlling only the average is provably insufficient:

Proposition 3.9. *There exists no function $f: \mathbb{R}^+ \rightarrow \mathbb{R}^+$ such that $D_{\text{KL}}^{\text{tok}, \max} \leq f(D_{\text{KL}}^{\text{seq}})$ for all policy pairs.*

Proof. Let c^* occur with probability p under π_{roll} , with $D_{\text{KL}}(c^*) = 1$ and $D_{\text{KL}}(c) = 0$ for $c \neq c^*$. Then $D_{\text{KL}}^{\text{tok}, \max} = 1$ while $D_{\text{KL}}^{\text{seq}} = p \rightarrow 0$ as $p \rightarrow 0$. \square

KL and TV routes are complementary. The KL route (Pinsker on marginal KL) gives sublinear context-shift scaling but is lossy in the advantage factor. The TV route gives a tight advantage factor but only linear context-shift scaling. The per-position crossover in the hybrid Adaptive bound B_{Adap}^* (Eq. (20)) automatically selects the tighter route at each position: the Pinsker route dominates for early positions (large remaining horizon $T-t$), while the coupling route dominates for late positions (small $T-t$) or when $\epsilon \ll \sqrt{\delta/2}$.

4 Trust Region Masking

4.1 Why Token-Level Methods Fail

Since the approximation error depends on $D_{\text{KL}}^{\text{tok,max}}$ (or $D_{\text{TV}}^{\text{tok,max}}$), controlling it requires a *sequence-level* intervention. Standard token-level methods fail for two structural reasons.

PPO clipping leaks gradients. PPO [Schulman et al., 2017] constrains updates via clipping: $L^{\text{CLIP}} = \mathbb{E}[\sum_t \min(\rho_t A_t, \text{clip}(\rho_t, 1 - \epsilon, 1 + \epsilon) A_t)]$. The clipping is asymmetric: when $\rho_t \gg 1 + \epsilon$ and $A_t < 0$, the objective uses the unclipped $\rho_t A_t$. In standard RL, this correctly penalizes over-represented bad actions. Under implementation divergence, the large ρ_t reflects numerical noise (e.g., MoE routing flip where $\pi_{\text{roll}}(v) = 0.9$ but $\pi_\theta(v) = 0.001$, giving $\rho \approx 900$), producing a massive erroneous gradient.

Token masking preserves vacuous bounds. Zeroing the gradient of outlier tokens (where $|\log \rho_t| > \tau$) prevents immediate gradient explosion but does not change the underlying divergence $D_{\text{KL}}^{\text{tok,max}}$ between π_{roll} and π_θ . The trust region remains violated:

Proposition 4.1. *Let $\mathcal{T}_{\text{mask}}$ be a token-level masking operator. Then*

$$D_{\text{KL}}^{\text{tok,max}}(\pi_\theta, \pi_{\text{roll}}) = D_{\text{KL}}^{\text{tok,max}}(\mathcal{T}_{\text{mask}}(\pi_\theta), \pi_{\text{roll}}).$$

Token masking modifies the optimization direction but does not restore the monotonic improvement guarantee.

The root cause is that the approximation error is cumulative over the sequence. If *any* token violates the trust region, the entire trajectory is compromised as an estimator for $J(\pi_\theta)$, and the entire sequence must be excluded.

4.2 The Masked Surrogate Objective

We define a binary sequence mask $M(x, y) = \mathbb{I}[(x, y) \in \text{Trust Region}]$ and the masked surrogate:

$$L_{\text{masked}}(\pi_\theta) = \mathbb{E}_{\pi_{\text{roll}}} \left[M(x, y) \cdot A(x, y) \cdot \sum_{t=1}^T \rho_t \right]. \quad (22)$$

The gradient is normalized by the *total* batch size N (not the accepted count), so rejected sequences contribute zero gradient. This is a rejection sampling mechanism: we choose not to learn from trajectories where off-policy divergence renders the gradient unreliable.

4.3 Masking Criterion and Implementation

Exact KL computation. Because π_{roll} logits are stored during rollout and π_θ logits are computed during the training forward pass, $D_{\text{KL}}(c_t)$ is computed exactly—over the full vocabulary—at no extra inference cost:

$$D_{\text{KL}}(c_t) = \sum_{v \in \mathcal{V}} \pi_{\text{roll}}(v|c_t) \log \frac{\pi_{\text{roll}}(v|c_t)}{\pi_\theta(v|c_t)}. \quad (23)$$

Max-based criterion: $M(x, y) = \mathbb{I}[\max_t D_{\text{KL}}(c_t) \leq \delta]$, directly bounding $D_{\text{KL}}^{\text{tok,max}}$. The threshold δ is *length-invariant*: it does not depend on T .

Combined criterion: In practice, combining max and average constraints ($\frac{1}{T} \sum_t D_{\text{KL}}(c_t) \leq \delta_{\text{avg}}$) allows looser individual thresholds while maintaining robustness.

Sample-based approximation. When full logits are unavailable, we recommend $k_2(\rho) = \frac{1}{2}(\log \rho)^2$ for max-filtering (symmetric, detects both $\rho \rightarrow 0$ and $\rho \rightarrow \infty$) and $k_3(\rho) = \rho - 1 - \log \rho$ for averaging (unbiased: $\mathbb{E}_{\pi_{\text{roll}}}[k_3] = D_{\text{KL}}(\pi_{\text{roll}} \parallel \pi_\theta)$). See Appendix E.

Algorithm 1 Trust Region Masking (TRM)

Require: Threshold δ ; Batch $\mathcal{D} = \{(x^{(i)}, y^{(i)})\}_{i=1}^N$; Stored π_{roll} logits

- 1: **Forward Pass:** Compute π_θ logits on all data
 - 2: **for** each sequence i **do**
 - 3: Compute $D_{\text{KL}}(c_t^{(i)})$ for all t using stored π_{roll} and current π_θ logits
 - 4: $M_i \leftarrow \mathbb{I}[\max_t D_{\text{KL}}(c_t^{(i)}) \leq \delta]$
 - 5: **end for**
 - 6: **Backward Pass:** $\nabla L_{\text{masked}} \leftarrow \frac{1}{N} \sum_{i=1}^N M_i \cdot A^{(i)} \cdot \sum_t \rho_t^{(i)} \nabla \log \pi_\theta(y_t^{(i)} | c_t^{(i)})$
 - 7: **Update:** $\theta \leftarrow \theta + \alpha \cdot \nabla L_{\text{masked}}$
-

4.4 Theoretical Guarantee

Theorem 4.2 (TRM Guarantee). *Algorithm 1 with threshold δ satisfies:*

1. **Bounded divergence:** For all accepted sequences ($M_i = 1$), $\max_t D_{\text{KL}}(c_t^{(i)}) \leq \delta$.
2. **Length-invariant threshold:** δ does not depend on sequence length T .
3. **Non-vacuous error bound:** If additionally $D_{\text{KL}}^{\text{tok,max}} \leq \delta$ holds globally (for all reachable contexts), then:

$$|J(\pi_\theta) - J(\pi_{\text{roll}}) - L(\pi_\theta)| \leq B^*(\delta, \epsilon), \quad (24)$$

where B^* is the unified bound (Theorem 3.8) with $D_{\text{KL}}^{\text{tok,max}}$ replaced by δ . The condition $L(\pi_\theta) > B^*$ guarantees $J(\pi_\theta) > J(\pi_{\text{roll}})$.

Proof. Part (1) holds by construction of the masking criterion. Part (2) follows because the criterion $\max_t D_{\text{KL}}(c_t) \leq \delta$ depends only on the per-token maximum, not on T . Part (3): when $D_{\text{KL}}^{\text{tok,max}} \leq \delta$ globally, all bounds in Section 3 apply with $D_{\text{KL}}^{\text{tok,max}}$ replaced by δ , giving $|\text{Error}| \leq B^*$. Since $J(\pi_\theta) - J(\pi_{\text{roll}}) = L(\pi_\theta) + \text{Error} \geq L(\pi_\theta) - B^*$, the condition $L(\pi_\theta) > B^*$ ensures $J(\pi_\theta) > J(\pi_{\text{roll}})$. \square

Remark 4.3 (Role of masking). *The error bound involves the full surrogate L , while TRM computes the masked surrogate L_{masked} . TRM serves two complementary roles: (1) a high acceptance rate provides empirical evidence that $D_{\text{KL}}^{\text{tok,max}} \leq \delta$ holds globally, validating the precondition; (2) discarding mismatched trajectories avoids erroneous gradient updates, so $L_{\text{masked}} \approx L$ when acceptance is high. We recommend monitoring acceptance rates above 70%.*

Numerical illustration. At $T = 4096$, $\delta = 10^{-4}$, $\epsilon = 5 \times 10^{-3}$, $D_{\text{KL}}^{\text{seq}} = 0.01$, $D_{\text{TV}}^{\text{seq}} = 0.05$: the unified bound gives $B^* \leq 4.1$ (TV-Mixed), compared to the classical bound of 1677—a **409** \times improvement.

4.5 Experiments

We validate TRM on mathematical reasoning using Qwen3-8B-Base under Zero-RL setup [Guo et al., 2025], trained on deduplicated DAPO-MATH-17k and evaluated on AIME25. We use GRPO [Shao et al., 2024] with group size 16, batch size 32, and learning rate 1×10^{-6} . Evaluation uses Top-P= 0.95, Temperature= 1.0, reporting avg@32.

To simulate realistic mismatch, we use vLLM for inference and PyTorch FSDP for training. We measure the *Log Absolute Perplexity (PPL) Gap*:

$$\Delta_{\text{PPL}} = \frac{1}{N} \sum_{i=1}^N \left| \frac{1}{T_i} \sum_{t=1}^{T_i} \log \pi_{\theta}(y_t^{(i)} | c_t^{(i)}) - \frac{1}{T_i} \sum_{t=1}^{T_i} \log \pi_{\text{roll}}(y_t^{(i)} | c_t^{(i)}) \right|. \quad (25)$$

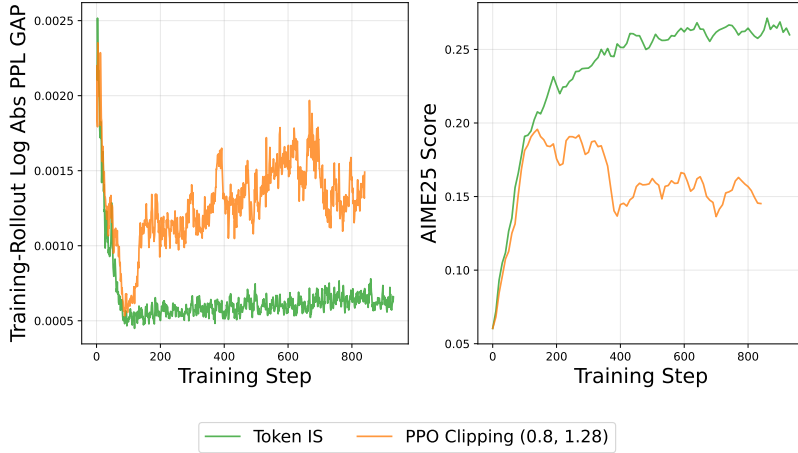


Figure 1: Token-level IS vs. PPO Clipping. Clipping exacerbates instability (larger PPL Gap, degraded score), confirming that token-level interventions cannot control $D_{\text{KL}}^{\text{tok,max}}$.

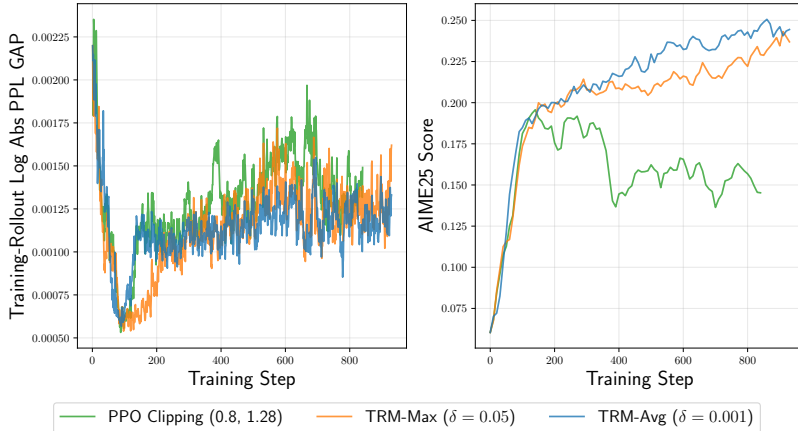


Figure 2: TRM vs. PPO Clipping. Both TRM-Max ($\delta = 0.05$) and TRM-Avg ($\delta = 0.001$) stabilize training, keeping the PPL Gap bounded.

Figure 1 confirms that token-level PPO clipping exacerbates instability. Figure 2 shows that both TRM variants maintain stability and consistent improvement on AIME25, keeping the PPL Gap bounded by rejecting mismatched sequences.

5 Conclusion

Off-policy mismatch is unavoidable in modern LLM-RL. We show that classical $O(T^2)$ trust region bounds are vacuous for long-horizon tasks and derive a family of tighter bounds—both KL-based

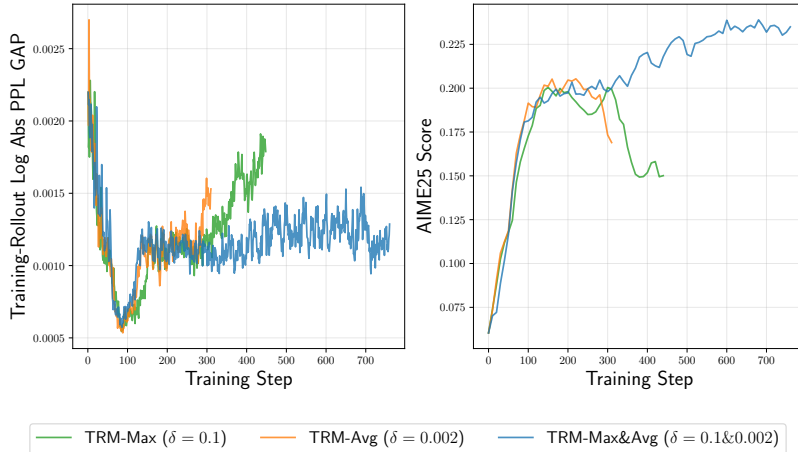


Figure 3: Combined criteria. Individually loose TRM-Max ($\delta=0.1$) and TRM-Avg ($\delta=0.002$) fail, but their combination succeeds—the max criterion catches outliers while the average criterion limits accumulated drift.

and TV-based—whose minimum yields the tightest known guarantee. The KL route provides sub-linear context-shift scaling; the TV route avoids Pinsker’s looseness. Their combination strictly dominates either alone. All bounds depend on the maximum token-level divergence, which cannot be controlled by token-level methods. Trust Region Masking enforces this constraint at the sequence level, enabling the first non-vacuous monotonic improvement guarantees for long-horizon LLM-RL. We discuss length-neutral extensions in Appendix F.

References

- Joshua Achiam, David Held, Aviv Tamar, and Pieter Abbeel. Constrained policy optimization. In *International conference on machine learning*, pages 22–31. PMLR, 2017.
- Samy Bengio, Oriol Vinyals, Navdeep Jaitly, and Noam Shazeer. Scheduled sampling for sequence prediction with recurrent neural networks. *Advances in neural information processing systems*, 28, 2015.
- Lasse Espeholt, Hubert Soyer, Remi Munos, Karen Simonyan, Vlad Mnih, Tom Ward, Yotam Doron, Vlad Firoiu, Tim Harley, Iain Dunning, et al. Impala: Scalable distributed deep-rl with importance weighted actor-learner architectures. In *International conference on machine learning*, pages 1407–1416. PMLR, 2018.
- Daya Guo, Dejian Yang, Haowei Zhang, Junxiao Song, Ruoyu Zhang, Runxin Xu, Qihao Zhu, Shirong Ma, Peiyi Wang, Xiao Bi, et al. Deepseek-r1: Incentivizing reasoning capability in llms via reinforcement learning. *arXiv preprint arXiv:2501.12948*, 2025.
- Sham Kakade and John Langford. Approximately optimal approximate reinforcement learning. In *Proceedings of the nineteenth international conference on machine learning*, pages 267–274, 2002.
- Woosuk Kwon, Zhuohan Li, Siyuan Zhuang, Ying Sheng, Lianmin Zheng, Cody Hao Yu, Joseph Gonzalez, Hao Zhang, and Ion Stoica. Efficient memory management for large language model

- serving with pagedattention. In *Proceedings of the 29th symposium on operating systems principles*, pages 611–626, 2023.
- Aixin Liu, Bei Feng, Bin Wang, Bingxuan Wang, Bo Liu, Chenggang Zhao, Chengqi Deng, Chong Ruan, Damai Dai, Daya Guo, et al. Deepseek-v2: A strong, economical, and efficient mixture-of-experts language model. *arXiv preprint arXiv:2405.04434*, 2024a.
- Fang Liu, Yang Liu, Lin Shi, Houkun Huang, Ruifeng Wang, Zhen Yang, Li Zhang, Zhongqi Li, and Yuchi Ma. Exploring and evaluating hallucinations in llm-powered code generation. *arXiv preprint arXiv:2404.00971*, 2024b.
- Jiacai Liu, Yingru Li, Yuqian Fu, Jiawei Wang, Qian Liu, and Yu Shen. When speed kills stability: Demystifying RL collapse from the training-inference mismatch, 2025. URL <https://richardli.xyz/rl-collapse>.
- Arun Nair, Praveen Srinivasan, Sam Blackwell, Cagdas Alcicek, Rory Fearon, Alessandro De Maria, Vedavyas Panneershelvam, Mustafa Suleyman, Charles Beattie, Stig Petersen, et al. Massively parallel methods for deep reinforcement learning. *arXiv preprint arXiv:1507.04296*, 2015.
- John Schulman, Sergey Levine, Pieter Abbeel, Michael Jordan, and Philipp Moritz. Trust region policy optimization. In *International conference on machine learning*, pages 1889–1897. PMLR, 2015.
- John Schulman, Filip Wolski, Prafulla Dhariwal, Alec Radford, and Oleg Klimov. Proximal policy optimization algorithms. *arXiv preprint arXiv:1707.06347*, 2017.
- Zhihong Shao, Peiyi Wang, Qihao Zhu, Runxin Xu, Junxiao Song, Xiao Bi, Haowei Zhang, Mingchuan Zhang, YK Li, Yang Wu, et al. Deepseekmath: Pushing the limits of mathematical reasoning in open language models. *arXiv preprint arXiv:2402.03300*, 2024.
- Noam Shazeer, Azalia Mirhoseini, Krzysztof Maziarz, Andy Davis, Quoc Le, Geoffrey Hinton, and Jeff Dean. Outrageously large neural networks: The sparsely-gated mixture-of-experts layer. *arXiv preprint arXiv:1701.06538*, 2017.
- Mohammad Shoeybi, Mostofa Patwary, Raul Puri, Patrick LeGresley, Jared Casper, and Bryan Catanzaro. Megatron-lm: Training multi-billion parameter language models using model parallelism. *arXiv preprint arXiv:1909.08053*, 2019.
- John Yang, Carlos E Jimenez, Alexander Wettig, Kilian Lieret, Shunyu Yao, Karthik Narasimhan, and Ofir Press. Swe-agent: Agent-computer interfaces enable automated software engineering. *Advances in Neural Information Processing Systems*, 37:50528–50652, 2024.
- Feng Yao, Liyuan Liu, Dinghuai Zhang, Chengyu Dong, Jingbo Shang, and Jianfeng Gao. Your efficient rl framework secretly brings you off-policy rl training, 2025. URL <https://fengyao.notion.site/off-policy-rl>.
- Weihao Zeng, Yuzhen Huang, Qian Liu, Wei Liu, Keqing He, Zejun Ma, and Junxian He. Simplerl-zoo: Investigating and taming zero reinforcement learning for open base models in the wild. *arXiv preprint arXiv:2503.18892*, 2025.
- Yanli Zhao, Andrew Gu, Rohan Varma, Liang Luo, Chien-Chin Huang, Min Xu, Less Wright, Hamid Shojanazeri, Myle Ott, Sam Shleifer, et al. Pytorch fsdp: experiences on scaling fully sharded data parallel. *arXiv preprint arXiv:2304.11277*, 2023.

Lianmin Zheng, Liangsheng Yin, Zhiqiang Xie, Chuyue Livia Sun, Jeff Huang, Cody Hao Yu, Shiyi Cao, Christos Kozyrakis, Ion Stoica, Joseph E Gonzalez, et al. Sglang: Efficient execution of structured language model programs. *Advances in neural information processing systems*, 37: 62557–62583, 2024.

Daniel M Ziegler, Nisan Stiennon, Jeffrey Wu, Tom B Brown, Alec Radford, Dario Amodei, Paul Christiano, and Geoffrey Irving. Fine-tuning language models from human preferences. *arXiv preprint arXiv:1909.08593*, 2019.

A Details on Off-Policy Mismatch in LLM-RL

A.1 Backend Discrepancies

Modern LLM-RL pipelines use separate stacks for inference and training:

Inference (vLLM/SGLang)	Training (Megatron/FSDP)
PagedAttention	FlashAttention-2
FP8/INT8 KV-cache quantization	BF16/FP32 accumulation
Aggressive operator fusion	Tensor parallelism

The root cause is floating-point non-associativity: $(a \oplus b) \oplus c \neq a \oplus (b \oplus c)$. Different parallel reduction orders in the softmax denominator yield slightly different results. While negligible for a single token, these errors compound autoregressively over T steps.

A.2 MoE Routing Discontinuities

In MoE models [Shazeer et al., 2017, Liu et al., 2024a], the output is $y = \sum_{i \in \mathcal{K}} g_i(x) \cdot E_i(x)$ where $\mathcal{K} = \text{Top-K}(h(x))$. The Top-K operator is discontinuous: if numerical jitter shifts $h_{\text{inf}} = h_{\text{train}} + \varepsilon$ such that $|h_{(K)} - h_{(K+1)}| < \|\varepsilon\|$, the selected experts change. This can cause $\pi_{\text{roll}}(v) = 0.9$ but $\pi_{\theta}(v) \approx 0.001$, producing importance ratio spikes $\rho \approx 900$.

A.3 Distributed Staleness

Actor-learner architectures [Espeholt et al., 2018, Nair et al., 2015] generate rollouts with θ_{old} while the learner updates to θ_{new} . A lag of k gradient steps ensures $\pi_{\text{roll}} \neq \pi_{\theta}$ even with identical implementations.

B Proofs of Foundational Lemmas

B.1 KL Chain Rule (Lemma B.1)

Lemma B.1 (KL Chain Rule). *For any time step t :*

$$D_{\text{KL}}(d_t^{\pi_{\text{roll}}} \| d_t^{\pi_{\theta}}) = \sum_{s=1}^{t-1} \mathbb{E}_{c_s \sim d_s^{\pi_{\text{roll}}}} [D_{\text{KL}}(c_s)]. \quad (26)$$

Proof. The joint trajectory distribution factorizes as:

$$d_t^{\pi}(x, y_{<t}) = P(x) \prod_{s=1}^{t-1} \pi(y_s | c_s). \quad (27)$$

Since $P(x)$ is shared, the KL divergence is:

$$D_{\text{KL}}(d_t^{\pi_{\text{roll}}} \| d_t^{\pi_{\theta}}) = \mathbb{E}_{(x, y_{<t}) \sim d_t^{\pi_{\text{roll}}}} \left[\log \frac{d_t^{\pi_{\text{roll}}}(x, y_{<t})}{d_t^{\pi_{\theta}}(x, y_{<t})} \right] \quad (28)$$

$$= \mathbb{E}_{d_t^{\pi_{\text{roll}}}} \left[\log \frac{P(x) \prod_{s=1}^{t-1} \pi_{\text{roll}}(y_s | c_s)}{P(x) \prod_{s=1}^{t-1} \pi_{\theta}(y_s | c_s)} \right] \quad (29)$$

$$= \mathbb{E}_{d_t^{\pi_{\text{roll}}}} \left[\sum_{s=1}^{t-1} \log \frac{\pi_{\text{roll}}(y_s | c_s)}{\pi_{\theta}(y_s | c_s)} \right] \quad (30)$$

$$= \sum_{s=1}^{t-1} \mathbb{E}_{d_t^{\pi_{\text{roll}}}} \left[\log \frac{\pi_{\text{roll}}(y_s | c_s)}{\pi_{\theta}(y_s | c_s)} \right]. \quad (31)$$

For each term in the sum, the expectation over $(x, y_{<t})$ under $d_t^{\pi_{\text{roll}}}$ can be decomposed. The log-ratio $\log(\pi_{\text{roll}}(y_s | c_s) / \pi_{\theta}(y_s | c_s))$ depends only on $(c_s, y_s) = (x, y_{\leq s})$. Marginalizing out y_{s+1}, \dots, y_{t-1} :

$$\mathbb{E}_{d_t^{\pi_{\text{roll}}}} \left[\log \frac{\pi_{\text{roll}}(y_s | c_s)}{\pi_{\theta}(y_s | c_s)} \right] = \mathbb{E}_{(x, y_{\leq s}) \sim d_{s+1}^{\pi_{\text{roll}}}} \left[\log \frac{\pi_{\text{roll}}(y_s | c_s)}{\pi_{\theta}(y_s | c_s)} \right] \quad (32)$$

$$= \mathbb{E}_{c_s \sim d_s^{\pi_{\text{roll}}}} \left[\mathbb{E}_{y_s \sim \pi_{\text{roll}}(\cdot | c_s)} \left[\log \frac{\pi_{\text{roll}}(y_s | c_s)}{\pi_{\theta}(y_s | c_s)} \right] \right] \quad (33)$$

$$= \mathbb{E}_{c_s \sim d_s^{\pi_{\text{roll}}}} [D_{\text{KL}}(c_s)]. \quad (34)$$

Substituting back into Eq. (31) completes the proof. \square

Corollary B.2. $D_{\text{KL}}(d_t^{\pi_{\text{roll}}} \| d_t^{\pi_{\theta}}) \leq (t-1) \delta$ and $D_{\text{KL}}^{\text{seq}} = \sum_{t=1}^T \mathbb{E}[D_{\text{KL}}(c_t)] \leq T\delta$.

Proof. Each summand satisfies $\mathbb{E}_{c_s} [D_{\text{KL}}(c_s)] \leq \max_{c_s} D_{\text{KL}}(c_s) \leq \delta$. \square

B.2 Martingale Property

Lemma B.3 (Martingale Property). *For any context c_t : $\mathbb{E}_{y_t \sim \pi_{\text{roll}}(\cdot | c_t)} [A_t^{\pi_{\text{roll}}}(c_t, y_t)] = 0$.*

Proof. Define $Q_t(c_t, y_t) := \mathbb{E}_{\pi_{\text{roll}}}[R | c_t, y_t]$ and $V_t(c_t) := \mathbb{E}_{\pi_{\text{roll}}}[R | c_t] = \mathbb{E}_{y_t \sim \pi_{\text{roll}}}[Q_t(c_t, y_t)]$. Then $A_t = Q_t - V_t$, so:

$$\mathbb{E}_{y_t \sim \pi_{\text{roll}}}[A_t(c_t, y_t)] = \mathbb{E}_{y_t \sim \pi_{\text{roll}}}[Q_t(c_t, y_t)] - V_t(c_t) = V_t(c_t) - V_t(c_t) = 0. \quad (35)$$

\square

B.3 Advantage Bound (Lemma 3.1)

Full proof. Using the Martingale Property:

$$g_t(c_t) = \mathbb{E}_{y_t \sim \pi_{\theta}}[A_t(c_t, y_t)] - \underbrace{\mathbb{E}_{y_t \sim \pi_{\text{roll}}}[A_t(c_t, y_t)]}_{=0} \quad (36)$$

$$= \sum_{y_t \in \mathcal{V}} (\pi_{\theta}(y_t | c_t) - \pi_{\text{roll}}(y_t | c_t)) \cdot A_t(c_t, y_t). \quad (37)$$

Bounding $|A_t|$: Since $R \in [0, 1]$, both $Q_t(c_t, y_t) = \mathbb{E}[R | c_t, y_t]$ and $V_t(c_t) = \mathbb{E}[R | c_t]$ lie in $[0, 1]$. Therefore $|A_t| = |Q_t - V_t| \leq 1$.

Hölder's inequality: Taking absolute values in Eq. (37):

$$|g_t(c_t)| \leq \sum_{y_t} |\pi_\theta(y_t|c_t) - \pi_{\text{roll}}(y_t|c_t)| \cdot |A_t(c_t, y_t)| \quad (38)$$

$$\leq \sum_{y_t} |\pi_\theta(y_t|c_t) - \pi_{\text{roll}}(y_t|c_t)| \cdot 1 \quad (39)$$

$$= 2 D_{\text{TV}}^{\text{tok}}(c_t). \quad (40)$$

Capping: Since $D_{\text{TV}}^{\text{tok}}(c_t) \leq 1$ for any pair of distributions, and by Pinsker's inequality $D_{\text{TV}}^{\text{tok}}(c_t) \leq \sqrt{D_{\text{KL}}(c_t)/2}$:

$$|g_t(c_t)| \leq 2 \min(1, \sqrt{D_{\text{KL}}(c_t)/2}). \quad (41)$$

Maximizing over c_t : $\|g_t\|_\infty \leq 2 \min(1, \epsilon, \sqrt{\delta/2})$. \square

B.4 Context Shift (Lemma 3.2)

Full proof. We establish each of the five bounds in Eq. (10).

Bound 1: Trivial. $D_{\text{TV}}(P, Q) \leq 1$ for any distributions P, Q .

Bound 2: Coupling. We prove $\|d_t^{\pi_\theta} - d_t^{\pi_{\text{roll}}}\|_{\text{TV}} \leq (t-1)\epsilon$ by induction.

Base case ($t=1$): $d_1^{\pi_\theta} = d_1^{\pi_{\text{roll}}} = P(x)$, so $D_{\text{TV}} = 0 = (1-1)\epsilon$.

Inductive step: Assume $\|d_t^{\pi_\theta} - d_t^{\pi_{\text{roll}}}\|_{\text{TV}} \leq (t-1)\epsilon$. The distribution at step $t+1$ is:

$$d_{t+1}^\pi(x, y_{\leq t}) = d_t^\pi(x, y_{<t}) \cdot \pi(y_t|c_t). \quad (42)$$

Using the triangle inequality for product distributions (coupling lemma):

$$\|d_{t+1}^{\pi_\theta} - d_{t+1}^{\pi_{\text{roll}}}\|_{\text{TV}} = \frac{1}{2} \sum_{x, y_{\leq t}} |d_t^{\pi_\theta}(c_t) \pi_\theta(y_t|c_t) - d_t^{\pi_{\text{roll}}}(c_t) \pi_{\text{roll}}(y_t|c_t)| \quad (43)$$

$$\begin{aligned} &\leq \frac{1}{2} \sum_{c_t, y_t} |d_t^{\pi_\theta}(c_t) - d_t^{\pi_{\text{roll}}}(c_t)| \cdot \pi_\theta(y_t|c_t) \\ &\quad + \frac{1}{2} \sum_{c_t, y_t} d_t^{\pi_{\text{roll}}}(c_t) \cdot |\pi_\theta(y_t|c_t) - \pi_{\text{roll}}(y_t|c_t)| \end{aligned} \quad (44)$$

$$= \|d_t^{\pi_\theta} - d_t^{\pi_{\text{roll}}}\|_{\text{TV}} \cdot \underbrace{\sum_{y_t} \pi_\theta(y_t|c_t)}_{=1} + \mathbb{E}_{c_t \sim d_t^{\pi_{\text{roll}}}} [D_{\text{TV}}^{\text{tok}}(c_t)] \quad (45)$$

$$\leq (t-1)\epsilon + \epsilon = t\epsilon. \quad (46)$$

In the last step, we used the inductive hypothesis and $D_{\text{TV}}^{\text{tok}}(c_t) \leq \epsilon$ for all c_t .

Bound 3: Pinsker on marginal KL. By the KL chain rule (Lemma B.1):

$$D_{\text{KL}}(d_t^{\pi_{\text{roll}}} \| d_t^{\pi_\theta}) = \sum_{s=1}^{t-1} \mathbb{E}_{c_s} [D_{\text{KL}}(c_s)] \leq (t-1)\delta. \quad (47)$$

Applying Pinsker's inequality to the marginal distributions:

$$\|d_t^{\pi_\theta} - d_t^{\pi_{\text{roll}}}\|_{\text{TV}} \leq \sqrt{\frac{D_{\text{KL}}(d_t^{\pi_{\text{roll}}} \| d_t^{\pi_\theta})}{2}} \leq \sqrt{\frac{(t-1)\delta}{2}}. \quad (48)$$

Bound 4: Data processing. Since d_t^π is a marginal of the full trajectory distribution $P^\pi(y|x)$ (obtained by marginalizing out y_t, \dots, y_T), the data processing inequality gives:

$$\|d_t^{\pi_\theta}(\cdot|x) - d_t^{\pi_{\text{roll}}}(\cdot|x)\|_{\text{TV}} \leq \|P^{\pi_\theta}(\cdot|x) - P^{\pi_{\text{roll}}}(\cdot|x)\|_{\text{TV}} = D_{\text{TV}}^{\text{seq}}. \quad (49)$$

Bound 5: Pinsker on sequence KL. Since $D_{\text{KL}}(d_t^{\pi_{\text{roll}}}\|d_t^{\pi_\theta}) \leq D_{\text{KL}}^{\text{seq}}$ (all summands in the chain rule are non-negative), Pinsker gives $D_{\text{TV}} \leq \sqrt{D_{\text{KL}}^{\text{seq}}/2}$.

Taking the minimum of all five bounds yields Eq. (10). \square

C Proofs of Main Theorems

All bounds start from the error decomposition (Eq. (9)):

$$|\text{Error}| \leq \sum_{t=1}^T 2\|g_t\|_\infty \cdot \|d_t^{\pi_\theta} - d_t^{\pi_{\text{roll}}}\|_{\text{TV}}, \quad (50)$$

which follows from $|\mathbb{E}_P[f] - \mathbb{E}_Q[f]| \leq 2\|f\|_\infty \cdot D_{\text{TV}}(P, Q)$ applied to each summand.

C.1 Pinsker-Marginal Bounds (Theorem 3.3)

KL variant. Use the advantage bound $\|g_t\|_\infty \leq 2\min(1, \sqrt{\delta/2})$ and the Pinsker context shift $\|d_t^{\pi_\theta} - d_t^{\pi_{\text{roll}}}\|_{\text{TV}} \leq \min(1, \sqrt{(t-1)\delta/2})$. Substituting into Eq. (50):

$$|\text{Error}| \leq \sum_{t=1}^T 2 \cdot 2\min\left(1, \sqrt{\frac{\delta}{2}}\right) \cdot \min\left(1, \sqrt{\frac{(t-1)\delta}{2}}\right) \quad (51)$$

$$= 4\min\left(1, \sqrt{\frac{\delta}{2}}\right) \sum_{t=1}^T \min\left(1, \sqrt{\frac{(t-1)\delta}{2}}\right) = B_{\text{PM}}^{\text{KL}}. \quad (52)$$

Small-divergence simplification. When $\delta \leq 2/T$: for all $t \leq T$, $(t-1)\delta/2 \leq (T-1)\delta/2 < 1$, so the context-shift cap is inactive. Also $\delta/2 < 1/T < 1$, so the advantage cap is inactive. Then:

$$B_{\text{PM}}^{\text{KL}} = 4\sqrt{\frac{\delta}{2}} \sum_{t=1}^T \sqrt{\frac{(t-1)\delta}{2}} = 4 \cdot \frac{\delta}{2} \sum_{k=0}^{T-1} \sqrt{k}. \quad (53)$$

The sum is bounded by the integral: $\sum_{k=0}^{T-1} \sqrt{k} \leq \int_0^T \sqrt{x} dx = \frac{2}{3}T^{3/2}$. Therefore:

$$B_{\text{PM}}^{\text{KL}} \leq 4 \cdot \frac{\delta}{2} \cdot \frac{2}{3}T^{3/2} = \frac{4}{3}T^{3/2}\delta. \quad (54)$$

Verification at $T = 4096$, $\delta = 10^{-4}$: $\frac{4}{3} \times (4096)^{3/2} \times 10^{-4} = \frac{4}{3} \times 262144 \times 10^{-4} = 34.95 \approx 35.0$.

TV variant. Replace the advantage bound with $\|g_t\|_\infty \leq 2\min(1, \epsilon)$, keeping the Pinsker context shift unchanged:

$$B_{\text{PM}}^{\text{TV}} = 4\min(1, \epsilon) \sum_{t=1}^T \min\left(1, \sqrt{\frac{(t-1)\delta}{2}}\right). \quad (55)$$

In the small-divergence regime: $B_{\text{PM}}^{\text{TV}} = 4\epsilon \cdot \sqrt{\delta/2} \cdot \frac{2}{3}T^{3/2} = \frac{8}{3}T^{3/2}\epsilon\sqrt{\delta/2}$.

Verification at $T = 4096$, $\delta = 10^{-4}$, $\epsilon = 5 \times 10^{-3}$: $\frac{8}{3} \times 262144 \times 5 \times 10^{-3} \times \sqrt{5 \times 10^{-5}} = \frac{8}{3} \times 262144 \times 5 \times 10^{-3} \times 7.07 \times 10^{-3} = 24.7$.

Note: when $\epsilon = \sqrt{\delta/2}$ (Pinsker tight), $B_{\text{PM}}^{\text{TV}} = B_{\text{PM}}^{\text{KL}}$. The TV variant is strictly tighter only when $\epsilon < \sqrt{\delta/2}$. \square

C.2 Mixed Bounds (Theorem 3.4)

KL variant. The marginal KL at any step t is bounded by the full sequence KL:

$$D_{\text{KL}}(d_t^{\pi_{\text{roll}}} \| d_t^{\pi_{\theta}}) = \sum_{s=1}^{t-1} \mathbb{E}[D_{\text{KL}}(c_s)] \leq \sum_{s=1}^T \mathbb{E}[D_{\text{KL}}(c_s)] = D_{\text{KL}}^{\text{seq}}. \quad (56)$$

The inequality holds because all summands are non-negative. Applying Pinsker:

$$\|d_t^{\pi_{\theta}} - d_t^{\pi_{\text{roll}}}\|_{\text{TV}} \leq \min\left(1, \sqrt{\frac{D_{\text{KL}}^{\text{seq}}}{2}}\right). \quad (57)$$

This bound is uniform in t . Summing over T steps with the KL advantage bound:

$$|\text{Error}| \leq \sum_{t=1}^T 2 \cdot 2 \min\left(1, \sqrt{\frac{\delta}{2}}\right) \cdot \min\left(1, \sqrt{\frac{D_{\text{KL}}^{\text{seq}}}{2}}\right) \quad (58)$$

$$= 4T \cdot \min\left(1, \sqrt{\frac{\delta}{2}}\right) \cdot \min\left(1, \sqrt{\frac{D_{\text{KL}}^{\text{seq}}}{2}}\right) = B_{\text{Mix}}^{\text{KL}}. \quad (59)$$

When both caps are inactive: $B_{\text{Mix}}^{\text{KL}} = 4T \sqrt{\delta/2} \sqrt{D_{\text{KL}}^{\text{seq}}/2} = 2T \sqrt{\delta \cdot D_{\text{KL}}^{\text{seq}}}$.

Verification at $T = 4096$, $\delta = 10^{-4}$, $D_{\text{KL}}^{\text{seq}} = 0.01$: $2 \times 4096 \times \sqrt{10^{-4} \times 0.01} = 8192 \times 10^{-3} = 8.192 \approx 8.2$.

TV variant. Use the TV advantage bound $\|g_t\|_{\infty} \leq 2 \min(1, \epsilon)$ and the data-processing context shift $\|d_t^{\pi_{\theta}} - d_t^{\pi_{\text{roll}}}\|_{\text{TV}} \leq \min(1, D_{\text{TV}}^{\text{seq}})$:

$$B_{\text{Mix}}^{\text{TV}} = 4T \cdot \min(1, \epsilon) \cdot \min(1, D_{\text{TV}}^{\text{seq}}). \quad (60)$$

Validity of the TV context-shift bound. The distribution $d_t^{\pi}(\cdot|x)$ over (y_1, \dots, y_{t-1}) is a marginal of the full trajectory distribution $P^{\pi}(\cdot|x)$ over (y_1, \dots, y_T) . By the data processing inequality for total variation, marginalization cannot increase TV distance:

$$\|d_t^{\pi_{\theta}}(\cdot|x) - d_t^{\pi_{\text{roll}}}(\cdot|x)\|_{\text{TV}} \leq \|P^{\pi_{\theta}}(\cdot|x) - P^{\pi_{\text{roll}}}(\cdot|x)\|_{\text{TV}} = D_{\text{TV}}^{\text{seq}}. \quad (61)$$

When caps are inactive: $B_{\text{Mix}}^{\text{TV}} = 4T\epsilon D_{\text{TV}}^{\text{seq}}$.

Verification at $T = 4096$, $\epsilon = 5 \times 10^{-3}$, $D_{\text{TV}}^{\text{seq}} = 0.05$: $4 \times 4096 \times 5 \times 10^{-3} \times 0.05 = 16384 \times 2.5 \times 10^{-4} = 4.096 \approx 4.1$.

When $\epsilon = \sqrt{\delta/2}$ and $D_{\text{TV}}^{\text{seq}} = \sqrt{D_{\text{KL}}^{\text{seq}}/2}$: $B_{\text{Mix}}^{\text{TV}} = 4T \sqrt{\delta/2} \sqrt{D_{\text{KL}}^{\text{seq}}/2} = 2T \sqrt{\delta D_{\text{KL}}^{\text{seq}}} = B_{\text{Mix}}^{\text{KL}}$. \square

C.3 Coupling Bound (Theorem 3.5)

Use the TV advantage bound $\|g_t\|_{\infty} \leq 2 \min(1, \epsilon)$ and the coupling context shift $\|d_t^{\pi_{\theta}} - d_t^{\pi_{\text{roll}}}\|_{\text{TV}} \leq \min(1, (t-1)\epsilon)$:

$$|\text{Error}| \leq \sum_{t=1}^T 2 \cdot 2 \min(1, \epsilon) \cdot \min(1, (t-1)\epsilon) = 4 \min(1, \epsilon) \sum_{t=1}^T \min(1, (t-1)\epsilon) = B_{\text{Coup}}. \quad (62)$$

Regime analysis. Define $t^* = \lceil 1/\epsilon \rceil + 1$ as the position where the cap activates.

Case 1: $T\epsilon \leq 1$ (small divergence). All caps are inactive ($t^* > T$):

$$B_{\text{Coup}} = 4\epsilon \cdot \epsilon \sum_{k=0}^{T-1} k = 4\epsilon^2 \cdot \frac{T(T-1)}{2} = 2T(T-1)\epsilon^2. \quad (63)$$

This recovers the classical bound.

Case 2: $T\epsilon > 1$ (large divergence). Split the sum at t^* :

$$\sum_{t=1}^T \min(1, (t-1)\epsilon) = \epsilon \sum_{k=0}^{t^*-2} k + (T - t^* + 1) \quad (64)$$

$$\leq \epsilon \cdot \frac{(1/\epsilon)^2}{2} + T = \frac{1}{2\epsilon} + T. \quad (65)$$

So $B_{\text{Coup}} \leq 4\epsilon(T + 1/(2\epsilon)) = 4T\epsilon + 2$. For large T : $B_{\text{Coup}} = O(T\epsilon)$.

Verification at $T = 4096$, $\epsilon = 7.07 \times 10^{-3}$ (Pinsker-derived): $1/\epsilon = 141.4$, so $t^* = 142$. Sum $= 7.07 \times 10^{-3} \times \frac{141 \times 142}{2} + (4096 - 142) = 70.8 + 3954 = 4024.8$. $B_{\text{Coup}} = 4 \times 7.07 \times 10^{-3} \times 4024.8 = 113.8$. \square

D Proof of the Adaptive Bound (Theorem 3.6)

The Adaptive bound uses an alternative error decomposition based on importance ratios rather than the Performance Difference Identity. We develop the proof in four steps.

D.1 Step 1: Exact Error Identity

Lemma D.1 (Exact Error Identity).

$$J(\pi_\theta) - J(\pi_{\text{roll}}) = L'_{\pi_{\text{roll}}}(\pi_\theta) - \Delta, \quad (66)$$

where:

$$\Delta := \mathbb{E}_{y \sim \pi_{\text{roll}}} \left[R(y) \sum_{t=1}^T (\rho_t - 1) \left(1 - \prod_{j=t+1}^T \rho_j \right) \right]. \quad (67)$$

Proof. We use the telescoping identity for products. For any sequence (ρ_1, \dots, ρ_T) :

$$\prod_{t=1}^T \rho_t - 1 = \sum_{t=1}^T (\rho_t - 1) \prod_{j=t+1}^T \rho_j. \quad (68)$$

Proof of Eq. (68): Write $\prod_{t=1}^T \rho_t = \rho_1 \cdot \prod_{j=2}^T \rho_j$. Then:

$$\prod_{t=1}^T \rho_t - 1 = (\rho_1 - 1) \prod_{j=2}^T \rho_j + \left(\prod_{j=2}^T \rho_j - 1 \right). \quad (69)$$

Applying the same decomposition recursively to $\prod_{j=2}^T \rho_j - 1$, and continuing, yields Eq. (68).

Now, the true performance difference is:

$$J(\pi_\theta) - J(\pi_{\text{roll}}) = \mathbb{E}_{y \sim \pi_{\text{roll}}} \left[R(y) \left(\prod_{t=1}^T \rho_t - 1 \right) \right] \quad (70)$$

$$= \mathbb{E}_{y \sim \pi_{\text{roll}}} \left[R(y) \sum_{t=1}^T (\rho_t - 1) \prod_{j>t} \rho_j \right]. \quad (71)$$

The surrogate is $L'_{\pi_{\text{roll}}}(\pi_\theta) = \mathbb{E}_{y \sim \pi_{\text{roll}}}[R(y) \sum_t (\rho_t - 1)]$. Subtracting:

$$J(\pi_\theta) - J(\pi_{\text{roll}}) - L'_{\pi_{\text{roll}}}(\pi_\theta) = \mathbb{E}_{y \sim \pi_{\text{roll}}} \left[R(y) \sum_t (\rho_t - 1) \left(\prod_{j>t} \rho_j - 1 \right) \right] \quad (72)$$

$$= -\mathbb{E}_{y \sim \pi_{\text{roll}}} \left[R(y) \sum_t (\rho_t - 1) \left(1 - \prod_{j>t} \rho_j \right) \right] = -\Delta. \quad (73)$$

Therefore Error = $J(\pi_\theta) - J(\pi_{\text{roll}}) - L'(\pi_\theta) = -\Delta$, and $|\text{Error}| = |\Delta|$. \square

D.2 Step 2: Tower Property Factorization

Define for each t :

$$A_t := |\rho_t - 1|, \quad B_t := \left| 1 - \prod_{j=t+1}^T \rho_j \right|. \quad (74)$$

Since $|R(y)| \leq 1$, the triangle inequality gives:

$$|\Delta| \leq \mathbb{E}_{y \sim \pi_{\text{roll}}} \left[\sum_{t=1}^T A_t \cdot B_t \right] = \sum_{t=1}^T \mathbb{E}_{y \sim \pi_{\text{roll}}} [A_t \cdot B_t]. \quad (75)$$

The factor A_t depends on (c_t, y_t) , while B_t depends on $y_{>t} = (y_{t+1}, \dots, y_T)$. They are *not* independent given c_t (since $c_{t+1} = (c_t, y_t)$ determines the future). We apply the tower property by conditioning on c_{t+1} :

$$\mathbb{E}_{y \sim \pi_{\text{roll}}} [A_t \cdot B_t] = \mathbb{E}_{c_{t+1} \sim d_{t+1}^{\pi_{\text{roll}}}} [\mathbb{E}_{y_t | c_t} [A_t | c_{t+1}] \cdot \mathbb{E}_{y_{>t} | c_{t+1}} [B_t]]. \quad (76)$$

Wait—since A_t is determined by (c_t, y_t) and $c_{t+1} = (c_t, y_t)$, conditioning on c_{t+1} makes A_t deterministic. More precisely:

$$\mathbb{E}_{y \sim \pi_{\text{roll}}} [A_t \cdot B_t] = \mathbb{E}_{y_{\leq t} \sim \pi_{\text{roll}}} [A_t \cdot \mathbb{E}_{y_{>t} \sim \pi_{\text{roll}}(\cdot | c_{t+1})} [B_t]]. \quad (77)$$

Now we compute the inner expectation. For fixed c_{t+1} :

$$\mathbb{E}_{y_{>t} \sim \pi_{\text{roll}}(\cdot | c_{t+1})} [B_t] = \mathbb{E}_{y_{>t} \sim \pi_{\text{roll}}} \left[\left| 1 - \prod_{j=t+1}^T \frac{\pi_\theta(y_j | c_j)}{\pi_{\text{roll}}(y_j | c_j)} \right| \right] \quad (78)$$

$$= \mathbb{E}_{y_{>t} \sim \pi_{\text{roll}}} \left[\left| 1 - \frac{P^{\pi_\theta}(y_{>t} | c_{t+1})}{P^{\pi_{\text{roll}}}(y_{>t} | c_{t+1})} \right| \right] \quad (79)$$

$$= \sum_{y_{>t}} P^{\pi_{\text{roll}}}(y_{>t} | c_{t+1}) \left| 1 - \frac{P^{\pi_\theta}(y_{>t} | c_{t+1})}{P^{\pi_{\text{roll}}}(y_{>t} | c_{t+1})} \right| \quad (80)$$

$$= \sum_{y_{>t}} |P^{\pi_{\text{roll}}}(y_{>t} | c_{t+1}) - P^{\pi_\theta}(y_{>t} | c_{t+1})| \quad (81)$$

$$= 2 D_{\text{TV}}(P^{\pi_{\text{roll}}}(\cdot | c_{t+1}) \| P^{\pi_\theta}(\cdot | c_{t+1})). \quad (82)$$

This is the total variation distance between the future-trajectory distributions.

For the outer factor, we expand the expectation over (c_t, y_t) :

$$\mathbb{E}_{y_{\leq t} \sim \pi_{\text{roll}}}[A_t] = \mathbb{E}_{c_t \sim d_t^{\pi_{\text{roll}}}}[\mathbb{E}_{y_t \sim \pi_{\text{roll}}(\cdot|c_t)}[\rho_t - 1]]. \quad (83)$$

We compute the inner expectation:

$$\mathbb{E}_{y_t \sim \pi_{\text{roll}}(\cdot|c_t)} \left[\left| \frac{\pi_{\theta}(y_t|c_t)}{\pi_{\text{roll}}(y_t|c_t)} - 1 \right| \right] = \sum_{y_t} \pi_{\text{roll}}(y_t|c_t) \left| \frac{\pi_{\theta}(y_t|c_t)}{\pi_{\text{roll}}(y_t|c_t)} - 1 \right| \quad (84)$$

$$= \sum_{y_t} |\pi_{\theta}(y_t|c_t) - \pi_{\text{roll}}(y_t|c_t)| \quad (85)$$

$$= 2 D_{\text{TV}}^{\text{tok}}(c_t). \quad (86)$$

Therefore:

$$\mathbb{E}_{y_{\leq t}}[A_t] = 2 \mathbb{E}_{c_t \sim d_t^{\pi_{\text{roll}}}}[D_{\text{TV}}^{\text{tok}}(c_t)] = 2 \bar{D}_t. \quad (87)$$

D.3 Step 3: Bounding the Future-Trajectory TV

We bound $D_{\text{TV}}(P^{\pi_{\text{roll}}}(\cdot|c_{t+1}) \| P^{\pi_{\theta}}(\cdot|c_{t+1}))$ for any fixed c_{t+1} . The future trajectory has $T - t$ steps.

Route A (Trivial):

$$D_{\text{TV}}(P^{\pi_{\text{roll}}}(\cdot|c_{t+1}) \| P^{\pi_{\theta}}(\cdot|c_{t+1})) \leq 1. \quad (88)$$

Route B (Pinsker + KL chain rule): By Pinsker's inequality applied to the future joint distribution:

$$D_{\text{TV}} \leq \sqrt{\frac{1}{2} D_{\text{KL}}(P^{\pi_{\text{roll}}}(\cdot|c_{t+1}) \| P^{\pi_{\theta}}(\cdot|c_{t+1}))}. \quad (89)$$

The conditional future KL decomposes via the chain rule:

$$D_{\text{KL}}(P^{\pi_{\text{roll}}}(\cdot|c_{t+1}) \| P^{\pi_{\theta}}(\cdot|c_{t+1})) = \sum_{k=t+1}^T \mathbb{E}_{c_k \sim \pi_{\text{roll}}(\cdot|c_{t+1})}[D_{\text{KL}}(c_k)] \quad (90)$$

$$\leq (T - t) \cdot \max_{k, c_k} D_{\text{KL}}(c_k) = (T - t) \delta. \quad (91)$$

Combining: $D_{\text{TV}} \leq \sqrt{(T - t)\delta/2}$.

Route C (Coupling): Applying the coupling argument to the $T - t$ remaining steps:

$$D_{\text{TV}}(P^{\pi_{\text{roll}}}(\cdot|c_{t+1}) \| P^{\pi_{\theta}}(\cdot|c_{t+1})) \leq (T - t) \epsilon. \quad (92)$$

This follows from the same inductive argument as the context-shift coupling bound, applied to the conditional future distributions.

Combined: Taking the minimum of all three routes:

$$D_{\text{TV}}(P^{\pi_{\text{roll}}}(\cdot|c_{t+1}) \| P^{\pi_{\theta}}(\cdot|c_{t+1})) \leq \min\left(1, (T - t) \epsilon, \sqrt{\frac{(T - t) \delta}{2}}\right). \quad (93)$$

Crucially, this bound holds for *every* realization of c_{t+1} , because the worst-case replacement in Eqs. (91)–(92) does not depend on the specific context. Therefore, the bound can be pulled outside the outer expectation over c_{t+1} .

D.4 Step 4: Combining the Factors

Substituting Eqs. (82), (87), and (93) into Eq. (77):

$$|\Delta| \leq \sum_{t=1}^T \mathbb{E}_{y_{\leq t}}[A_t] \cdot \sup_{c_{t+1}} 2D_{\text{TV}}(P^{\pi_{\text{roll}}}(\cdot|c_{t+1}) \| P^{\pi_{\theta}}(\cdot|c_{t+1})) \quad (94)$$

$$\leq \sum_{t=1}^T 2\bar{D}_t \cdot 2 \min\left(1, (T-t)\epsilon, \sqrt{\frac{(T-t)\delta}{2}}\right) \quad (95)$$

$$= 4 \sum_{t=1}^T \bar{D}_t \cdot \min\left(1, (T-t)\epsilon, \sqrt{\frac{(T-t)\delta}{2}}\right) = B_{\text{Adap}}^*. \quad (96)$$

This proves Eq. (20). The KL and TV variants (Eqs. (18)–(19)) follow by dropping one of the two non-trivial terms inside the min.

D.5 Step 5: Strictness over Prior Bounds

Recovery of $B_{\text{PM}}^{\text{KL}}$. Set $\bar{D}_t = \min(1, \sqrt{\delta/2})$ (worst-case per-position TV via Pinsker) and use only the Pinsker route for the future TV in $B_{\text{Adap}}^{\text{KL}}$:

$$B_{\text{Adap}}^{\text{KL}} = 4 \min\left(1, \sqrt{\frac{\delta}{2}}\right) \sum_{t=1}^T \min\left(1, \sqrt{\frac{(T-t)\delta}{2}}\right). \quad (97)$$

By the index substitution $k = T - t$ (so $t = T - k$, and k ranges from 0 to $T - 1$):

$$\sum_{t=1}^T \min\left(1, \sqrt{\frac{(T-t)\delta}{2}}\right) = \sum_{k=0}^{T-1} \min\left(1, \sqrt{\frac{k\delta}{2}}\right) = \sum_{t=1}^T \min\left(1, \sqrt{\frac{(t-1)\delta}{2}}\right). \quad (98)$$

This is exactly the sum in $B_{\text{PM}}^{\text{KL}}$ (Eq. (12)), confirming $B_{\text{Adap}}^{\text{KL}}|_{\bar{D}_t = \sqrt{\delta/2}} = B_{\text{PM}}^{\text{KL}}$.

Recovery of B_{Coup} . Set $\bar{D}_t = \epsilon$ and use only the coupling route in $B_{\text{Adap}}^{\text{TV}}$:

$$B_{\text{Adap}}^{\text{TV}} = 4\epsilon \sum_{t=1}^T \min(1, (T-t)\epsilon) = 4\epsilon \sum_{k=0}^{T-1} \min(1, k\epsilon) = B_{\text{Coup}}. \quad (99)$$

Strict improvement. Since $\bar{D}_t \leq \min(1, \epsilon, \sqrt{\delta/2})$ always, and strict inequality $\bar{D}_t < \epsilon$ or $\bar{D}_t < \sqrt{\delta/2}$ holds whenever the per-position divergence is non-uniform, the Adaptive bounds are strictly tighter than their PM/Coupling counterparts whenever divergence is non-uniform across positions.

Additionally, B_{Adap}^* with the per-position min over coupling and Pinsker routes is at least as tight as $\min(B_{\text{Adap}}^{\text{KL}}, B_{\text{Adap}}^{\text{TV}})$, since the per-position minimum is at most the global minimum of the two sums. \square

D.6 Crossover Analysis

The hybrid bound B_{Adap}^* selects between two routes for the future TV at each position. The crossover occurs where $(T-t)\epsilon = \sqrt{(T-t)\delta/2}$, i.e., $(T-t) = \delta/(2\epsilon^2)$.

When Pinsker is tight ($\epsilon = \sqrt{\delta/2}$): crossover at $T - t = 1$. The Pinsker route is tighter for all but the last position, and the hybrid reduces to $B_{\text{Adap}}^{\text{KL}}$.

When Pinsker is loose ($\epsilon \ll \sqrt{\delta/2}$): crossover at $T - t = \delta/(2\epsilon^2) \gg 1$. The coupling route wins for positions near the end (small $T-t$), while Pinsker wins for early positions (large $T-t$). The hybrid interpolates, providing significant improvement over either route alone.

E Sample-Based Estimators (k_2 and k_3)

When storing full logits is infeasible, we use sample-based estimators from $\rho_t = \pi_\theta(y_t|c_t)/\pi_{\text{roll}}(y_t|c_t)$.

k_3 for averaging: $f(\rho) = \rho - 1 - \log \rho$. This is the unique estimator satisfying $\mathbb{E}_{y_t \sim \pi_{\text{roll}}}[k_3(\rho_t)] = D_{\text{KL}}(\pi_{\text{roll}}(\cdot|c_t) \parallel \pi_\theta(\cdot|c_t))$ exactly, verified by:

$$\mathbb{E}_{\pi_{\text{roll}}}[\rho - 1 - \log \rho] = \mathbb{E}_{\pi_{\text{roll}}}\left[\frac{\pi_\theta}{\pi_{\text{roll}}} - 1\right] - \mathbb{E}_{\pi_{\text{roll}}}\left[\log \frac{\pi_\theta}{\pi_{\text{roll}}}\right] = (1 - 1) + \mathbb{E}_{\pi_{\text{roll}}}\left[\log \frac{\pi_{\text{roll}}}{\pi_\theta}\right] = D_{\text{KL}}. \quad (100)$$

It is non-negative ($k_3 \geq 0$ by Jensen’s inequality) and asymmetric (penalizes $\rho \gg 1$ more than $\rho \ll 1$).

k_2 for max-filtering: $f(\rho) = \frac{1}{2}(\log \rho)^2$. This is symmetric: $k_2(\rho) = k_2(1/\rho)$. It detects both support collapse ($\rho \rightarrow 0$) and impulse noise ($\rho \rightarrow \infty$) equally, which is essential for the max-based criterion. Note k_2 is biased as an estimator of D_{KL} but serves as a robust outlier detector.

The rigorous guarantees of Theorem 4.2 hold only with exact KL from full logits.

F Length-Neutral Trust Region Masking

F.1 Length Bias in TRM

While TRM’s threshold δ is length-invariant, the *rejection probability* increases with T . Under a simplifying i.i.d. assumption with per-token violation probability p :

$$\Pr[\text{accept}] = (1 - p)^T \approx e^{-pT}. \quad (101)$$

This decays exponentially in T , systematically rejecting long sequences. For reasoning tasks where correct solutions often require longer chains of thought, this bias is concerning.

F.2 Length-Neutral TRM (LN-TRM)

Motivated by the Adaptive bound, we define a trajectory-level error score:

$$W(y) := \sum_{t=1}^T |\rho_t - 1| \cdot w_t, \quad w_t := \min\left(1, (T-t)\epsilon, \sqrt{\frac{(T-t)\delta}{2}}\right), \quad (102)$$

and normalize by the weight sum $Z(T) := \sum_{t=1}^T w_t$ (precomputable). The masking criterion is:

$$M(y) = \mathbb{I}\left[\widetilde{W}(y) := W(y)/Z(T) \leq \delta_W\right]. \quad (103)$$

Since \widetilde{W} is a *weighted average* of $|\rho_t - 1|$, it is approximately length-invariant.

Proposition F.1 (LN-TRM Guarantee). *If $D_{\text{KL}}^{\text{tok,max}} \leq \delta$ globally, then $|\text{Error}| \leq 2 \mathbb{E}_{\pi_{\text{roll}}}[W(y)]$. For accepted trajectories, $W(y) \leq \delta_W \cdot Z(T)$.*

Proof. From the Adaptive bound proof (Step 4): $|\text{Error}| \leq 2 \sum_t \mathbb{E}[|\rho_t - 1|] \cdot w_t = 2 \mathbb{E}[W(y)]$ by linearity of expectation (since w_t is deterministic). For accepted sequences, $\widetilde{W}(y) \leq \delta_W$ gives $W(y) \leq \delta_W \cdot Z(T)$. \square

F.3 Simplified Variant: Sequence-Error Ratio (SER)

For minimal implementation overhead:

$$W_{\text{SER}}(y) := \frac{1}{T} \sum_{t=1}^T |\rho_t - 1|, \quad M(y) = \mathbb{I}[W_{\text{SER}}(y) \leq \delta_{\text{SER}}]. \quad (104)$$

This adds three lines to any GRPO/PPO implementation:

```
W = mean(abs(rho - 1), dim=-1) # per-sequence average
M = (W <= delta_ser).float()   # binary mask
loss = loss * M                # mask rejected sequences
```

SER connects to the linear bound via $\mathbb{E}[|\rho_t - 1|] = 2D_{\text{TV}}^{\text{tok}}(c_t)$: controlling $W_{\text{SER}} \leq \delta$ bounds the per-trajectory error at rate $O(T\delta)$. Since W_{SER} is an average, its variance decreases as $O(1/\sqrt{T})$ by CLT, making SER mildly biased *in favor of* longer sequences. We recommend $\delta_{\text{SER}} \in [0.03, 0.10]$.

Table 2: Length bias properties of masking methods.

Method	Criterion	Rejection scaling	Guarantee
TRM-Max	$\max_t D_{\text{KL}}(c_t) \leq \delta$	$1 - (1 - p)^T$ (exponential)	Exact
TRM-Avg	$\frac{1}{T} \sum_t D_{\text{KL}}(c_t) \leq \delta$	\approx constant	Weaker (avg \neq max)
LN-TRM	$W(y) \leq \delta_W$	\approx constant	Up to $Z(T)$ factor
SER	$\frac{1}{T} \sum \rho_t - 1 \leq \delta$	\approx constant	Via linear bound